

Detecting colorectal cancer using electrical impedance spectroscopy: an *ex vivo* feasibility study

Angela Pathiraja¹, Paul Ziprin¹, Arsam Shiraz³, Reza Mirnezami¹,
Andrew Tizzard², Brian Brown⁴, Andreas Demosthenous³
and Richard Bayford^{2,3}
¹Imperial College London, UK
²Middlesex University, London, UK.
³University College London, UK.
⁴Sheffield University, UK.

Emails: angela.pathiraja12@imperial.ac.uk and r.bayford@mdx.ac.uk

ABSTRACT

Objective: Colorectal cancer is the fourth most common cancer worldwide, with a lifetime risk of around 20%. Current solutions do not allow clinicians to objectively assess tissue abnormality during endoscopy and perioperatively. A solution capable of objectively assessing samples in real time could greatly improve the treatment process. A solution that can be integrated in minimally invasive diagnostics and management strategies to provide real-time point-of-care information would be greatly transformative. Electrical impedance spectroscopy (EIS) may provide such a solution. In this paper, we present a feasibility study on using EIS in assessing colorectal tissue.

Approach: We performed tetrapolar EIS using ZedScan on excised human colorectal tumour tissue and the matched normal colonic mucosa in 22 freshly resected specimens following elective surgery for colorectal cancer. Histopathological examination was used to confirm the final diagnosis. Statistical significance was assessed with Wilcoxon signed rank test.

Main results: Tetrapolar EIS could discriminate cancer with statistically significant results when applying frequencies between 305 Hz – 625 kHz ($p < 0.05$). 300 Ω was set as the transfer impedance threshold to detect cancer. Thus, the area under the corresponding receiver operating characteristic curve for this threshold was 0.7105.

Significance: This feasibility study demonstrates that impedance spectra changes in colorectal cancer tissue are detectable and may be statistically significant, suggesting that EIS has the potential to be the core technology in a novel non-invasive point of care test for detecting colorectal cancer. These results warrant further development and increasing the size of the study with a device specificity designed for colorectal cancer.

Keywords: cancer, colorectal, electrical impedance spectroscopy (EIS), diagnosis, real-time

1 Introduction

Colorectal cancer (CRC) is a leading cause of global cancer-related mortality in men and women with over 1 million new cases diagnosed annually worldwide (Cunningham *et al.*, 2010). It is the fourth most common cancer worldwide, with a lifetime risk of around 20%. Complete surgical resection remains the only curative option for management of CRC and is combined with chemotherapy and/or radiotherapy in selected cases (Andre N *et al.*, 2005).

The past 30 years have seen a significant shift towards increasingly 'minimal access' surgical approaches (minimally invasive surgery, MIS), and laparoscopic surgical techniques are now routinely employed in the operative management of cancers of the colon (Jayne DG *et al.*, 2007) and rectum (Chand Chand M *et al.*, 2012). Endoluminal cancer excision is an extension of this philosophy and represents the next major objective on the MIS roadmap, offering a further reduction in surgical risks by permitting cancer lesion removal by completely 'scarless' means. Here, tumours are approached and removed via the bowel lumen using an operating endoscope, such as in endoscopic mucosal resection (Woodward TA *et al.*, 2012, Waye JD *et al.*, 2001) or a proctoscope in transanal endoscopic microsurgery (De Graaf EJ *et al.*, 2002). These approaches are technically demanding but appear to result in reduced post-operative morbidity (De Graaf EJ *et al.*, 2009).

Regardless of the intervention method, histopathological assessment of excised tissue samples for a definitive assessment of samples is an integral part of the process. However, as this assessment relies on various steps that take time (Loughrey *et al.*, 2014), it results in a substantial time delay prior to conclusive tissue diagnosis. Recent endeavours have aimed to provide more real-time information for clinicians. Examples of these are chromo-endoscopy, narrow-band imaging and, most recently, the intelligent knife (iKnife) (Mcgill *et al.*, 2013 and Balog *et al.*, 2013). However, a reliable, quantitative and tissue-sparing measure of tissue abnormality at initial endoscopy or intraoperative margin resection remains to be achieved. Of particular interest to our clinical work is the possibility of assessing and detecting cancer during endoscopic and surgical procedures as a predictor of recurrence, including lymph node involvement, poor differentiation, perineural invasion, and vascular invasion. Also of clinical importance is the possibility to predict negative distal resection margin and negative circumferential resection margins. This can be considered especially for locally-advanced poorly-differentiated rectal tumours which have undergone neoadjuvant (preoperative) chemoradiation therapy.

1.1 Electrical Impedance Spectroscopy (EIS)

In tetrapolar EIS, conventionally, a current signal of different frequencies is applied to two electrodes and the induced voltage signal is recorded across another two in the vicinity to measure a complex transfer-impedance. Given that biological tissue responds differently to different frequencies (Duck FA. 1990, Foster KR and Schwan HP 1989) and the impedance profile may be different for different tissues (Gabriel *et al.*, 1996), EIS may be used to quantitatively assess biological tissues. EIS may take less than a second if the target frequency range is kept relatively high. Thus, it may provide a real-time assessment.

The detection of cancer pathology in the tissue (specifically cervical cancer) using bioimpedance measurements has been reported in literature (S. Abdul *et al.*, 2005, Abdul *et al.*, 2006 and JA Tidy *et al.*, 2013). In these contributions, tetrapolar EIS measurements were performed on the wall of the cervix for the detection of cervical intraepithelial neoplasia, and the distinction from normal epithelium using a four-electrode portable probe.

A major advantage of the EIS approach would be the ability to provide real-time information regarding the state for the tissue, equivalent to a biopsy, without requiring any alteration to the tissue being measured. Moreover, as the EIS technology can be miniaturised, it could be integrated in the existing endoscopic and surgical technologies.

1.2 Competing Solutions

In recent years, several methods have been proposed for real-time intra-operative tumour margin assessment including diffusive reflectance (Wilke *et al*, 2009), radiofrequency-based detection (Allweis *et al*, 2008), targeted fluorescence imaging (Van Dam GM *et al*, 2011) and the iKnife (Mcgill *et al*, 2013 and Balog *et al*, 2013). Each of these techniques is subject to particular strengths and limitations. However, a general consensus has yet to be reached on the optimal strategy.

Table 1 compares various methods for intraoperative tumour margin assessment with our proposed approach.

Method	Advantage	Disadvantage
Radiofrequency-based detection (e.g. MarginProbe)	<ul style="list-style-type: none"> • Real-time measurement 	<ul style="list-style-type: none"> • Technology not small enough to mount on an endoscope • No evidence that it will work on colorectal (only studies have been on breast)
Real-time near infrared targeted fluorescence imaging	<ul style="list-style-type: none"> • Good sensitivity and specificity in tumour margin detection • Compatible with minimally invasive cancer therapy 	<ul style="list-style-type: none"> • Limited detection depth • Requires fluorescent conjugate to be injected intravenously
iKnife	<ul style="list-style-type: none"> • Gives instant reading in the form of a mass spec profile 	<ul style="list-style-type: none"> • Requires tissue ablation before measurement can be carried out
EIS	<ul style="list-style-type: none"> • Can detect surface as well as depth, highly suitable for CRC • Small physical size • Technology is low cost • Does not require tissue alteration in order to obtain measurements 	<ul style="list-style-type: none"> • Technology for effective characterisation of the colorectal tissue <u>does not currently exist</u>

Table 1: Comparison of Intraoperative Methods

In this paper we assess whether EIS could be used to differentiate colorectal cancer from benign colonic mucosa in an *ex vivo* study. In section 2, details of the experimental protocol and materials as well as the ensuing analyses are shown. This is followed by results, discussion and concluding remarks in sections 3, 4 and 5 respectively.

2 Materials and Methods:

We initially developed and validated our impedance measurement protocol on 10 test samples. Then we performed the experiments and analyses detailed in this section. Ethical approval was granted by the Coventry and Warwickshire REC -reference 13/WM/0320.

2.1 Surgical sample acquisition and preparation

Over a period of 6 months, 22 patients (17 males, median age 77, age range 48-85) diagnosed with an advanced-stage colon cancer due for surgical resection were prospectively recruited to the study, following informed consent on the day of surgery. Colorectal specimens, collected with an ischemic time of 20-45 minutes from surgical resection (dependent on the availability of the

histopathologist), were prepared in a standardised manner: an experienced histopathologist, opened the sample, pre-identified and marked the lesion and the surrounding normal bowel mucosa on the same specimen (Figure 1).

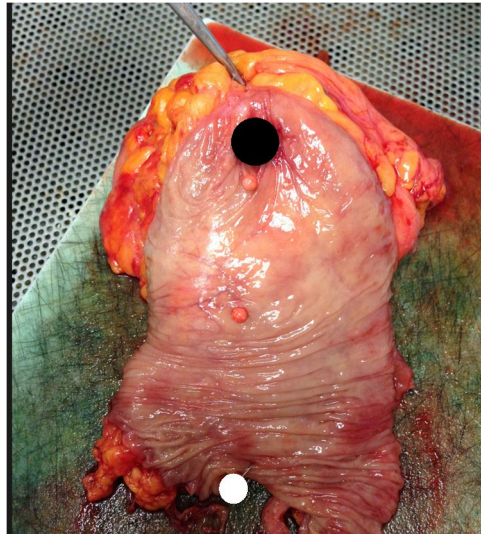


Figure 1: Fresh colorectal specimen with identified sites marked by pins (colorectal cancer lesion marked by black pin and normal mucosa marked by white pin).

2.2 EIS device and measurements

EIS measurements were made by applying sinusoidal current of 12 μA amplitude at fourteen different frequencies from 76 Hz to 625 kHz with the ZedScan device (Zilico Ltd, Manchester, UK) in test mode to the pre-identified sites in each case (i.e. lesion site and the matched normal mucosa). The ZedScan device at the tip of the sensing area consists of a square arrangement of 4 gold electrodes, each 1 mm in diameter where the adjacent electrodes are 1.65 mm apart. Each measurement was repeated at least 12 and up to 24 times depending on the time available to us before histopathological analysis and then all the measurements taken from a sample were averaged to provide a more accurate measure of its trans-impedance. The purpose of obtaining measurements with the ZedScan device was primarily to determine the range of frequencies required for colorectal cancer and to generally evaluate the viability of the concept. Throughout the measurement, the tissue remained in the sluice room, which is set at a temperature between 5-10 degrees Celsius.

2.3 Histopathological analysis

The two pre-identified areas (of the malignant lesion and normal mucosa) for each of the 22 samples subsequently underwent formal histopathological analysis as per the normal clinical protocol. This consisted of formalin fixation, tissue processing, sectioning and subsequent haematoxylin and eosin staining and cover-slipping, thereby enabling microscopic analysis and histopathological confirmation of tissue type (Loughrey *et al*, 2014). Histopathological statuses of the 22 tissue specimens were used as the ground truth for the status of the corresponding samples.

2.4 Data analysis

Each sample was allocated a sample number, and the patient and hospital-related information was kept strictly confidential (only the clinical research fellow conducting the study had access to this). This was done to anonymise all the data so that no patient-specific data could be identified. For each sample, the corresponding measurement data set was downloaded on a personal computer using the software supplied with the ZedScan device. The collected data, real and imaginary components of transfer impedance, was exported to Microsoft Excel software to appropriately arrange the data and then was imported in Matlab R2016b (The MathWorks, Inc., Natick,

Massachusetts, United States) and SPSS (IBM, UK) for analysis. As the recorded measurements were not normally distributed (as determined by Shapiro-Wilk test) the Wilcoxon rank sum test for paired non-parametric data of small sample sets was used to test for differences between matched normal and malignant tissue transfer impedance magnitudes at each frequency. A p-value less than 0.05 was considered statistically significant.

To plot a receiver operating characteristic (ROC) curve and measure the corresponding area under it (AUROC), the sensitivity and specificity at each of the 14 different frequencies were calculated to plot sensitivity (y-axis) versus 1-specificity (x-axis) for a range of cut-offs (100 Ω - 500 Ω). These were the transfer-impedance magnitude thresholds above, which a sample would classify as cancer at all frequencies. A natural logarithmic function was used to fit the ROC data points at each frequency for all the cut-offs and consequently AUROC was calculated in each case. 300 Ω was identified as the threshold that maximised the AUROC while having most of the data points on the upper left corner of the curve.

3 Results:

Data from 22 specimens were originally obtained. 3 specimens' data sets were excluded from final data analysis as 2 were found to have no residual microscopic evidence of cancer following chemoradiotherapy ("complete responders" – samples 13 and 18), and 1 was found to be non-malignant tissue ("benign villous adenoma" -sample 19) following formal histopathological assessment. This left 19 specimens for data analysis. Patient demographics and histopathological characteristics for each patient are summarized in Table 2.

Sample no.	Age	Sex	Site of Cancer	Type of Cancer	T stage	N stage	Ischaemic time
1	77	F	Rectosig.	Mod. diff. adenoCa	3	0	20
2	48	F	Rectum	Poorly diff. inv adenoCa	4	2	35
3	54	F	Sigmoid	Mod. diff. inv. adenoCa	1	0	15
4	40	M	Splen. Fl.	Poorly diff. adenoCa	3	0	45
5	78	M	Sigmoid	Mod. diff. adenoCa	4	0	30
6	55	M	Asc.col	Undifferentiated adenoCa	3	0	30
7	85	M	Caecum	Mod. diff. adenoCa	3	0	20
8	72	F	Caecum	Poorly diff. adenoCa.	4	2	20
9	73	M	Rectum	Mod. diff. adenoCa.	2	0	30
10	69	M	Rectum	Mod. diff. adenoCa	2	0	35
11	73	F	Rectosig.	Poorly diff. adenoCa	1	2	25
12	75	M	Caecum	Mod. diff. adenoCa	3	0	20
13	41	M	Rectum	COMPLETE RESPONDER	N/A	N/A	25
14	68	M	Asc.col	Mod.diff. inv.adenoCa	1	0	30
15	64	M	Rectum	Mod. diff. adenoCa	3	0	35
16	38	M	Asc. col	Poorly diff. adenoCa	4	1	45
17	79	M	Sigmoid	Mod. diff. adenoCa	3	0	30
18	72	M	Rectum	COMPLETE RESPONDER	N/A	N/A	20
19	69	M	Asc.col	VILLOUS ADENOMA	N/A	N/A	25
20	51	M	Rectum	Poorly diff. adenoCa	4	1	15
21	71	M	Rectum	Poorly diff. adenoCa	3	1	20
22	65	M	Rectum	Mod. diff. adenoCa	3	0	25

Table 2: Patient demographics and histopathological characteristics of the 22 specimens (Mod. = moderately, diff. = differentiated, inv. = invasive, adenoCa = adenocarcinoma)

The impedance spectra generally ranged from about 100 Ω to 1000 Ω over the 14 frequencies. Mean and median impedances for the indicated 19 cancer sites and the corresponding normal sites at each of the 14 different frequencies were calculated. The median magnitude and phase of impedances for the 19 cancer sites and those of the corresponding normal tissues as well as those of the 2 complete-responder-specimens are shown in Figure 2. In the 19 specimens under study, a difference between the impedance magnitude of cancer and the corresponding normal tissue is observed. In 15 out of 19 specimens cancer showed higher impedances than the corresponding normal tissues. As shown in Figure 2, the phase information shows a less significant difference.

Table 3 shows the median transfer-impedance magnitude values along with the interquartile ranges at each of the 14 varying frequencies for the 19 colorectal cancer lesions and the corresponding normal tissues. Wilcoxon rank sum test P-values for the differences in median impedances are also presented, with statistically significant P-values (<0.05) noted at frequencies between 305 Hz - 625 kHz.

Figure 3 shows the ROC curve. The area under the ROC curve (AUROC) was calculated to be 0.7105, (where the tool can produce a perfect discrimination between the two groups, AUROC is 1).

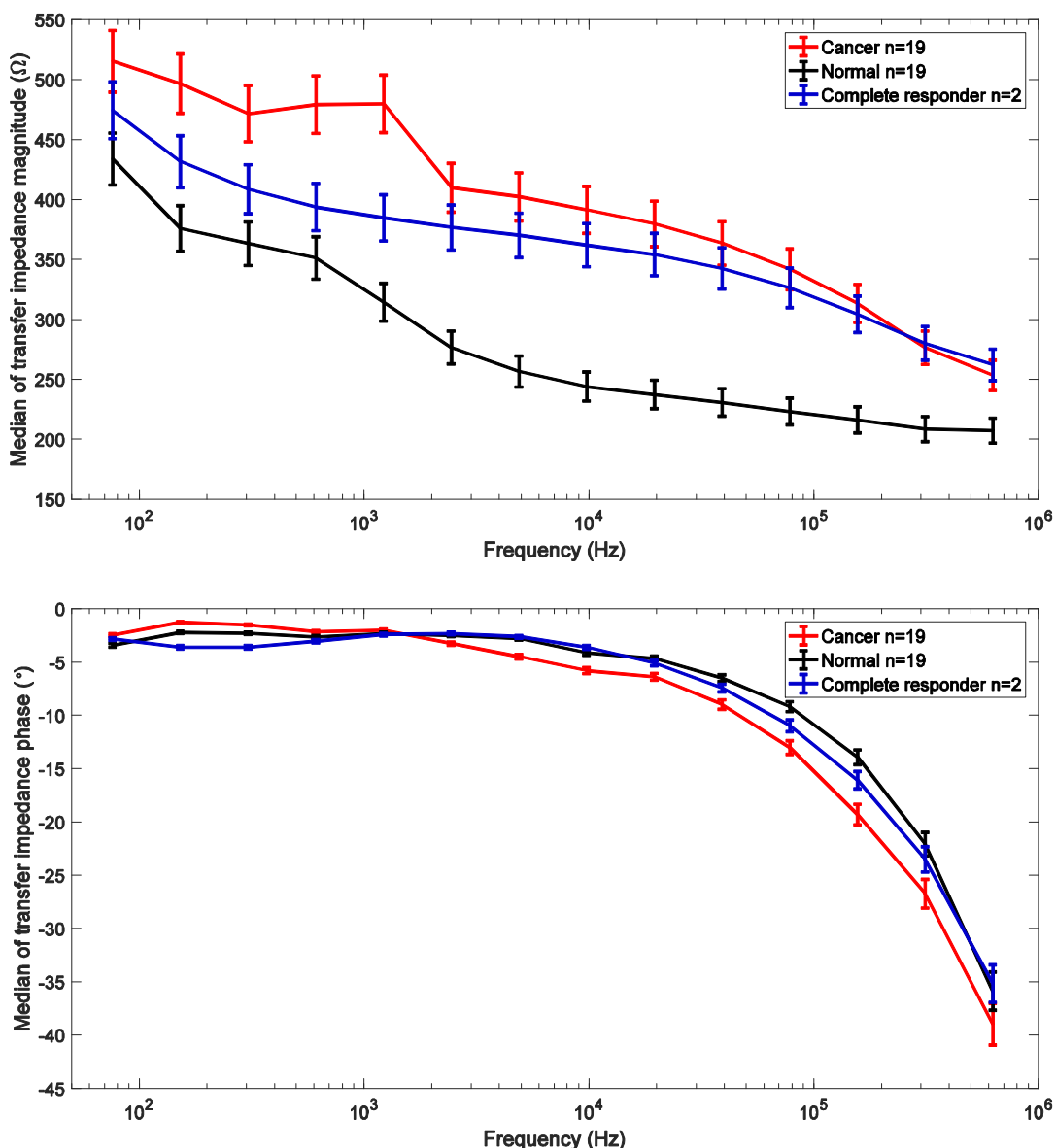


Figure 2: Median transfer-impedance magnitude and phase (with $\pm 5\%$ error bars) over 14 frequencies for 19 cancerous samples, 2 complete responder samples and 19 normal tissue samples.

Frequency (Hz)	Median (+ IQR) of impedances for 19 cancer lesions'	Median (+ IQR) of impedances for 19 benign lesions'	Wilcoxon rank sum test p-values
76	515 (350-974)	433 (283-616)	0.1149
152	496 (335-924)	376 (265-508)	0.0961
305	471 (325-911)	363 (257-434)	0.0471
610	479 (311-769)	351 (248-388)	0.0195
1220	480 (311-732)	314 (239-356)	0.0131
2441	409 (307-697)	276 (234-346)	0.0086
4882	402 (301-655)	256 (230-336)	0.0051
9765	391 (292-606)	244 (226-325)	0.0072
19531	379 (285-539)	237 (222-318)	0.0066
39062	363 (276-494)	230 (215-306)	0.0079
78125	341 (265-445)	223 (207-295)	0.0102
156250	313 (249-391)	216 (194-280)	0.0111
312500	276 (232-237)	208 (179-261)	0.0131
625000	253 (222-285)	207 (181-247)	0.0228

Table 3: Median impedance measures along with the interquartile ranges (IQR) for the 19 colorectal cancer (CRC) lesions and corresponding normal tissue. Wilcoxon rank sum test P-values for the differences in impedance have been stated.

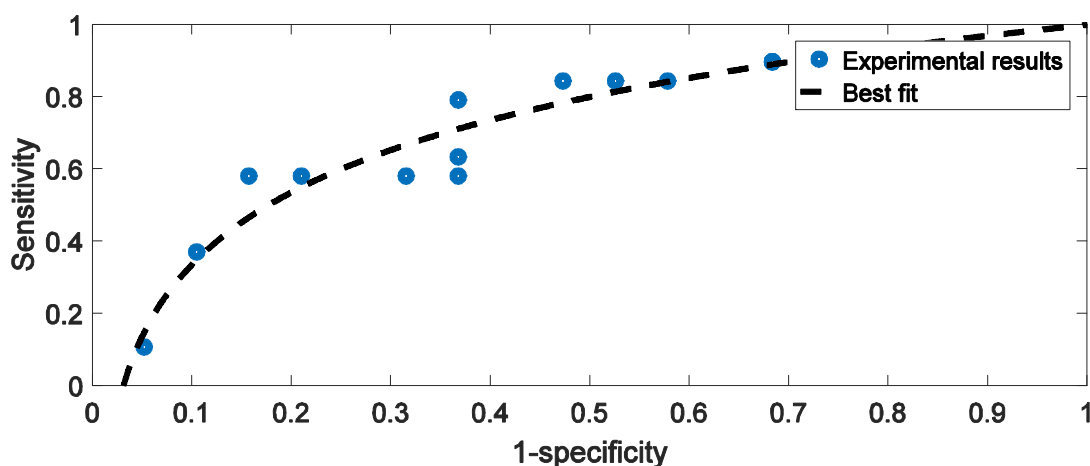


Figure 3: ROC curve comparing tissue analysed by the ZedScan probe as either malignant or normal CRC, based on the cut-off electrical impedance indicator of 300Ω (AUROC = 0.7105).

4 Discussion:

The purpose of our prospective ex-vivo pilot study was to evaluate whether bioimpedance technology would be able to discriminate between colorectal cancer tissue and normal colonic mucosa. The results presented here support other published data of larger studies, which report the effect of dysplastic changes of specific epithelial tissue on electrical impedance spectra (Brown

et al, 2000, Keshtkar *et al*, 2012, Mahara *et al*, 2015). Similarly, smaller studies looking at oesophageal cancers showed that oesophageal squamous epithelium also had much higher impedances than the dysplastic tissue and adenocarcinomas and squamous cell carcinomas (Knabe *et al*, 2013). Interestingly, our study of normal colonic columnar epithelium against colorectal adenocarcinomatous tissue showed that cancer in general had higher impedance than the normal columnar epithelium. Further work to compare the microscopic structure of the different types of colorectal tissue would facilitate further understanding of why these bioimpedance changes occur.

Although 15 of the 19 adenocarcinoma samples showed bioimpedance spectra that were uniformly higher, 4 of the 19 adenocarcinoma samples showed bioimpedance spectra that were lower than the normal colorectal tissue bioimpedance spectra. It is unclear why this was the case. However, it may reflect the fact that 3 of these were found to be poorly or undifferentiated adenocarcinomas, whereas the majority of the adenocarcinomas that showed higher bioimpedances were moderately differentiated adenocarcinomas. It may be that the lack of differentiation in tissue structure affects the electrical resistance and subsequent bioimpedance characteristics of these samples. However, more work needs to be done to investigate this hypothesis further.

Also of interest, the specimens where a complete pathological response was observed following chemoradiotherapy, demonstrated bioimpedance spectra that appear to have become similar to that of normal tissues. However, this was in a very small sample (n=2) and would need further investigation with more samples before any firm conclusions could be drawn.

Although our study presents promising results, there are limitations that should be addressed. It should be noted that our results are based on a small initial sample size of 22 surgically resected colorectal samples, of which 19 were histopathologically-proven colorectal cancer specimens. It is important to note that when a cancer case has chemoradiotherapy, this often renders the specimen free of any identifiable residual disease. Such samples are therefore excluded from our study and subsequently have a large impact on our final sample size that could be obtained. Additionally, although the ROC curve is a promising representation of our initial data, the specificities observed were moderate at the lower measured frequencies.

Our specimens were collected immediately after surgical resection, there was some delay between the tissue initially losing its blood supply and the EIS measurements being obtained - an ischaemic time. It is known that once *ex-vivo*, tissue cellular structure begins to change with increasing ischaemic times (Spruessel *et al*, 2004). Additionally, as malignant tissue is known to be highly vascularized, increasing ischaemic times may also result in dehydration of the tissue, which may in turn result in alteration of electrical conductivity and impedance measurement. Further work needs to be done to investigate the effect of ischaemic times on EIS measurements.

Finally, it is worth noting that whilst the Zedscan tool enabled us to make reproducible measurements of bioimpedance in colorectal tissue, it has been ergonomically designed for the specific measurement of cervical tissue at colposcopy. Consequently, whilst the long probe is required for application down a colposcope, conversely it prohibits stable measurement of colorectal tissue, as pressure effects on the tip can result in altered measurements (Keshtkar and Keshtkar, 2009). The future development of bioimpedance technology that is designed to facilitate more controlled measurements of colorectal tissue may result in more sensitive readings.

5 Conclusions

Our feasibility study is the first of its kind to show that EIS can discriminate between surgically resected colorectal cancer and normal colorectal mucosa in patients with confirmed colorectal cancer. This initial study on a small sample size warrants the need for the development of a custom-made EIS technology tailored for this application to perform a similar study on a much wider pathological range of colorectal samples as well as a miniaturised solution for *in vivo* tests. We hope that the concept may be developed into an EIS probe that could be deployed down the

working channel of an endoscope or integrated into robotic surgical tools to provide a real-time virtual biopsy and diagnosis of colorectal cancer.

Acknowledgements:

We would like to thank Peter Highfield from Zilico Ltd for the continued support throughout this study. Dr Angela Pathiraja received a National Institute of Health Research Academic Clinical fellowship (2013-16), which enabled her to set up and conduct this study.

This study was undertaken with ethical approval, reference 135339.

Reference List

Cunningham D, Atkin W, Lenz HJ, Lynch HT, Minsky B, Nordlinger B, et al. Colorectal cancer. *Lancet*. 2010; **375**(9719): 1030-47. Andre N et al., *Gut*. 2005; **54**(8): 1194-202.

Andre N, Schmiegel W. Chemoradiotherapy for colorectal cancer. *Gut*. 2005; **54**(8): 1194-202.

Jayne DG, Guillou PJ, Thorpe H, Quirke P, Copeland J, Smith AM, et al. Randomized trial of laparoscopic-assisted resection of colorectal carcinoma: 3-year results of the UK MRC CLASICC Trial Group. *J Clin Oncol*. 2007; **25**(21): 3061-8.

Chand M, Bhoday J, Brown G, Moran B, Parvaiz A. Laparoscopic surgery for rectal cancer. *J R Soc Med*. 2012; **105**(10): 429-35.

Woodward TA, Heckman MG, Cleveland P, De Melo S, Raimondo M, Wallace M. Predictors of complete endoscopic mucosal resection of flat and depressed gastrointestinal neoplasia of the colon. *Am J Gastroenterol*. 2012; **107**(5): 650-4.

Waye JD. Endoscopic mucosal resection of colon polyps. *Gastrointest Endosc Clin N Am*. 2001; **11**(3): 537-48, vii.

De Graaf EJ, Doornebosch PG, Stassen LP, Debets JM, Tetteroo GW, Hop WC. Transanal endoscopic microsurgery for rectal cancer. *Eur J Cancer*. 2002; **38**(7): 904-10.

De Graaf EJ, Doornebosch PG, Tollenaar RA, Meershoek-Klein Kranenbarg E, de Boer AC, Bekkering FC, et al. Transanal endoscopic microsurgery versus total mesorectal excision of T1 rectal adenocarcinomas with curative intention. *Eur J Surg Oncol*. 2009; **35**(12): 1280-5.

McGill SK, Evangelou E, Ioannidis JP et al. Narrow band imaging to differentiate neoplastic and non-neoplastic colorectal polyps in real time: a meta-analysis of diagnostic operating characteristics. *Gut*. 2013; **62**(12): 1704-13.

Balog J, Sasi-Szabo L, Kinross J et al. Intraoperative tissue identification using rapid evaporative ionization mass spectrometry. *Science translational medicine*. 2013; **5**(194): 194ra93.

Loughrey MB, Quirke P, Shepherd NA. Dataset for colorectal cancer histopathology reports. 3 ed. London: Royal College of Pathologists; 2014.

S. Abdul, B. H. Brown, P. Milnes, and J. A. Tidy, "A clinical study of the use of impedance spectroscopy in the detection of cervical intraepithelial neoplasia (CIN)," *Gynecologic Oncology*, vol. 99, pp. S64-S66, 2005.

S. Abdul, B. H. Brown, P. Milnes, and J. A. Tidy, "The use of electrical impedance spectroscopy in the detection of cervical intraepithelial neoplasia," *Int. J. Gynecol. Cancer*, vol. 16, pp. 1823-1832, 2006.

JA Tidy, BH Brown, TJ Healey, S Daayana, M Martin, W Prendiville, HC Kitchener. (2013) Accuracy of detection of high-grade cervical intraepithelial neoplasia using electrical impedance spectroscopy with colposcopy *Br J Obstet Gynae* 120; 400-411.

Duck FA. Physical properties of tissue. London: Academic Press, 1990.

Foster KR, Schwan HP. Dielectric properties of tissues and biological materials: a critical review. *Crit Rev Biomed Eng* 1989; 17:25–104.

Gabriel S, Lau WR and Gabriel C. The dielectric properties of biological tissues: III. Parametric models for the dielectric spectrum of tissues. *Physics in Medicine and Biology*. 1996; 41 (11): 2271

Wilke LG, Brown JQ, Bydlon TM, Kennedy SA, Richards LM, Junker MK, et al. Rapid noninvasive optical imaging of tissue composition in breast tumor margins. *Am J Surg*. 2009; **198**(4): 566-74.

Allweis TM, Kaufman Z, Lelcuk S, Pappo I, Karni T, Schneebaum S, et al. A prospective, randomized, controlled, multicenter study of a real-time, intraoperative probe for positive margin detection in breast-conserving surgery. *Am J Surg*. 2008; **196**(4): 483-9.

Van Dam GM, Themelis G, Crane LM, Harlaar NJ, Pleijhuis RG, Kelder W, et al. Intraoperative tumor-specific fluorescence imaging in ovarian cancer by folate receptor-alpha targeting: first in-human results. *Nat Med*. 2011; **17**(10): 1315-9.

Brown BH, Tidy JA, Boston K et al. Relation between tissue structure and imposed electrical current flow in cervical neoplasia. *Lancet*. 2000;355(9207):892-5.

Keshtkar A, Salehnia Z, Keshtkar A et al. Bladder cancer detection using electrical impedance technique (tabriz mark 1). *Patholog Res Int*. 2012;2012:470101.

Mahara A, Khan S, Murphy E et al. 3D Microendoscopic Electrical Impedance Tomography for Margin Assessment during Robot-Assisted Laparoscopic Prostatectomy. *IEEE Trans Med Imaging*. 2015.

Knabe M, Kurz C, Knoll T, et al. Diagnosing early Barrett's neoplasia and oesophageal squamous cell neoplasia by bioimpedance spectroscopy in human tissue. *United European Gastroenterol J*. 2013;1(4):236-41.

Spruessel, Steinmann, Jung et al. Tissue ischaemia time affects gene and protein expression patterns within minutes following surgical tumour excision. *BioTechnique* 2004; 36: 1030-1037

Keshtkar A and Keshtkar A. Probe Pressure optimization in Bio-impedance spectroscopy. *World Congress on Medical Physics and Biomedical Engineering*. 2009.